

## Localized mechanical stress induces time-dependent actin cytoskeletal remodeling and stiffening in cultured airway smooth muscle cells

Linhong Deng,<sup>1</sup> Nigel J. Fairbank,<sup>1</sup> Ben Fabry,<sup>2</sup> Paul G. Smith,<sup>3</sup> and Geoffrey N. Maksym<sup>1</sup>

<sup>1</sup>School of Biomedical Engineering, Dalhousie University, Halifax, Nova Scotia, Canada B3H 3J5;

<sup>2</sup>Physiology Program, Harvard School of Public Health, Boston, Massachusetts 02115; and

<sup>3</sup>Pediatrics Department, Case Western Reserve University, Cleveland, Ohio 44106

Submitted 2 September 2003; accepted in final form 2 April 2004

**Deng, Linhong, Nigel J. Fairbank, Ben Fabry, Paul G. Smith, and Geoffrey N. Maksym.** Localized mechanical stress induces time-dependent actin cytoskeletal remodeling and stiffening in cultured airway smooth muscle cells. *Am J Physiol Cell Physiol* 287: C440–C448, 2004. First published April 7, 2004; 10.1152/ajpcell.00374.2003.—Mechanical stress (MS) causes cytoskeletal (CSK) and phenotypic changes in cells. Such changes in airway smooth muscle (ASM) cells might contribute to the pathophysiology of asthma. We have shown that periodic mechanical strain applied to cultured ASM cells alters the structure and expression of CSK proteins and increases cell stiffness and contractility (Smith PG, Moreno R, and Ikebe M. *Am J Physiol Lung Cell Mol Physiol* 272: L20–L27, 1997; and Smith PG, Deng L, Fredberg JJ, and Maksym GN. *Am J Physiol Lung Cell Mol Physiol* 285: L456–L463, 2003). However, the mechanically induced CSK changes, altered cell function, and their time courses are not well understood. Here we applied MS to the CSK by magnetically oscillating ferrimagnetic beads bound to the CSK. We quantified CSK remodeling by measuring actin accumulation at the sites of applied MS using fluorescence microscopy. We also measured CSK stiffness using optical magnetic twisting cytometry. We found that, during MS of up to 120 min, the percentage of beads associated with actin structures increased with time. At 60 min,  $68.1 \pm 1.6\%$  of the beads were associated with actin structures compared with only  $6.7 \pm 2.8\%$  before MS and  $38.4 \pm 5.5\%$  in time-matched controls ( $P < 0.05$ ). Similarly, CSK stiffness increased more than twofold in response to the MS compared with time-matched controls. These changes were more pronounced than observed with contractile stimulation by 80 mM KCl or  $10^{-4}$  M acetylcholine. Together, these findings imply that MS is a potent stimulus to enhance stiffness and contractility of ASM cells through CSK remodeling, which may have important implications in airway narrowing and dilation in asthma.

mechanical stress; actin cytoskeleton; stiffness; airway smooth muscle cell; optical magnetic twisting cytometry; airway constriction and dilation; asthma

THE ABILITY FOR A CELL TO remodel and change its cytoskeleton (CSK) is essential for cell migration and is an important feature of smooth muscle function. Mechanical stress (MS) influences remodeling of the CSK and can lead to altered cellular function (16, 23). In the airways, it is the airway smooth muscle (ASM) cells that are ultimately responsible for airway narrowing in response to bronchoconstricting agonists, and it is thought that changes in the ASM cell structure and function may be contributing factors to the pathophysiology of asthma. Many changes associated with asthma may affect ASM cell structure and function, including inflammatory chemical mediators, airway remodeling, and changes in extracellular matrix compo-

sition, that affect both loading and signaling to the ASM (3, 5). Less studied are the effects on the ASM cell of MS that is prevalent in the airways and, in all likelihood, elevated in asthma and bronchial hyperresponsiveness due to coughing, wheezing, increased inspiratory efforts, increased tone, and exacerbation. Because of the central role that ASM plays in airway narrowing, force transmission, and possibly in limiting airway dilation, it is important to understand how the CSK and its stiffness may be mechanically regulated in ASM (29).

Our laboratory has previously reported that cultured ASM cells exposed to chronic (up to 12 days) cyclic mechanical strain exhibited increased stiffness, CSK reorganization, increased shortening capacity, and increased contractility and force production (32, 34, 36, 38). Mechanically strained cells also exhibit increased proliferation, increased velocity of shortening, and calcium sensitivity (35, 37, 38). These changes are consistent with bronchial hyperresponsiveness in vivo (6, 12, 24). Indeed, increased proliferation and altered contractile and biochemical characteristics have been observed in cells harvested from asthmatic subjects (5).

These mechanically induced changes in ASM cells have been documented for cells experiencing mechanical stimulation for 10–12 days. On the other hand, it is known that CSK is a dynamic structure in a variety of cell types (11) and can respond to MS on a much shorter time scale through remodeling and typically causing increases in cell stiffness (10, 16, 17), thus approaching changes that have been observed when stimulated with contractile agonist. However, the effect of MS on ASM cells remains not well understood, especially during its acute application. Changes in CSK structure in ASM cells due to MS have only been qualitatively examined during chronically applied stress (34). Furthermore, although changes in CSK proteins induced by contractile activation have been studied (21, 26), structural changes were not examined, and it is not known how this compares with mechanically induced effects. Therefore, we investigated the response of the CSK structure in ASM cells to localized acute MS and its time course, as well as how the induced changes in CSK structure translate into altered mechanical function in terms of the CSK stiffness.

### MATERIALS AND METHODS

**Cell culture.** Canine ASM cells in culture were prepared as follows. Trachealis muscle was harvested and digested in collagenase and elastase with soy trypsin inhibitor, as previously described (35, 37).

Address for reprint requests and other correspondence: G. N. Maksym, School of Biomedical Engineering, Dalhousie Univ., 5981 Univ. Ave., Halifax, NS, Canada B3H 3J5 (E-mail: geoff.maksym@dal.ca).

The costs of publication of this article were defrayed in part by the payment of page charges. The article must therefore be hereby marked “advertisement” in accordance with 18 U.S.C. Section 1734 solely to indicate this fact.

Freshly dissociated cells were seeded into flasks at a density of  $5 \times 10^4$  cells/cm<sup>2</sup> in a mixture medium of DMEM and Ham's F-12 (1:1) (Invitrogen, Burlington, ON) with supplements of 10% FBS, 100 U/ml of penicillin, and 100 µg/ml streptomycin. Medium was changed every 2–4 days, and the cells were passaged when they grew to confluence (10–14 days) before being used for experiment. We used cells of passages 3–5 for experiments in this study. Cells were serum deprived and supplemented with 5.7 µg/ml insulin and 5 µg/ml transferrin for 24 h before the experiment. The cells were harvested by brief exposure to 0.05% trypsin and 1 mM EDTA and plated onto either glass microscopic coverslips (12-mm diameter; Fisher Scientific, Nepean, ON) or 96-well format plastic wells (6.4-mm diameter Costar Stripwell; Corning, Corning, NY), depending on the type of assessment (see below). Before cell plating, the coverslips and plastic wells were coated with type I collagen (Cohesion Technologies, Palo Alto, CA) at 25 and 5 µg/ml, respectively, for at least 24 h at 4°C.

**Magnetic twisting stimulator.** We developed a device known as a magnetic twisting stimulator (MTS) (Fig. 1) to deliver localized MS to the CSK of cultured ASM cells by magnetically oscillating ferrimagnetic beads that were bound avidly to the CSK. Details of this technique have been published previously (8, 41). In brief, the beads were permanently magnetized and then twisted in a homogeneous magnetic field of varying amplitude and direction that was generated by a solenoid.

The ferrimagnetic beads (4.5-µm diameter, kindly provided by Dr. J. J. Fredberg, Harvard School of Public Health, Cambridge, MA) were coated with a synthetic RGD (Arg-Gly-Asp)-containing peptide (Peptide 2000; Integra Life Sciences, San Diego, CA) at a concentration of 50 µg peptide/mg beads in 1-ml carbonate buffer (pH 9.4) and stored at 4°C. Before use, the RGD-coated beads were washed and resuspended in DMEM/F-12 medium with 1% BSA. Then the beads were deposited onto the cultured ASM cells prepared on 12-mm coverslips at a density of  $62 \times 10^3$  beads/cm<sup>2</sup> (~70,000 beads per coverslip). The RGD coating of the beads enabled them to bind specifically to transmembrane integrin receptors on the apical cell surface, forming focal adhesions, whereas the BSA in the bead suspension blocked nonspecific binding. At 15 min, the binding between the beads and cells was well established (22, 25, 41), and unbound beads were washed away. The cell-bead preparations were then placed inside the solenoid coil of the MTS. The beads were first magnetized in the horizontal direction by a large-amplitude but short-duration electric pulse (~2 kV, 250 µs) through a pair of Helmholtz coils, which provided a field of >0.1 tesla. Then a current source delivered a small sinusoidal current (~1 A) through a vertically oriented solenoid coil to generate a varying magnetic field,

applying an oscillating torque to the magnetized beads (Fig. 1). The specific torque ( $T$ ) is defined as the mechanical torque per unit bead volume and is given by

$$T = cH \cos \theta \quad (1)$$

where  $H$  is the magnetic twisting field,  $\theta$  is the angle between the magnetic moment of the bead and the original magnetization direction, and  $c$  is the bead constant (1.65 Pa/G), determined by measuring the angular velocity while twisting the beads in a standard fluid of known viscosity (40). Because  $\theta$  is usually small (<4°) (25), the specific torque closely follows  $H$ .  $H$  was set to amplitude of 34 G at 0.3 Hz, thus applying a specific torque at amplitude of 56 Pa at approximately breathing frequency. This corresponds to applied MS on the order of 1,000 Pa, depending on bead-cell contact area and cell thickness, as previously determined computationally (27).

The solenoid and the culture dishes were located in an incubator (Sanyo) so that the cells were maintained at 37°C in humidified air containing 5% CO<sub>2</sub> while being mechanically stimulated. An electric fan was placed below the twisting coil to generate a moderate airflow for removing excess heat that resulted from resistive losses in the solenoid coil.

**Fluorescence microscopy.** We used fluorescence microscopy to visualize the actin CSK of ASM cells of the cell-bead preparations on 12-mm glass coverslips. Filamentous actin was labeled with fluorescently conjugated phalloidin (Alexa 488; Molecular Probes, Eugene, OR). These preparations were either exposed to mechanical stimulation or used as time-matched controls. At different time points (0, 5, 15, 30, 60, and 120 min) after the initial 15 min of bead binding to the cells, the cells on the coverslip were washed with PBS and fixed in a solution containing 4% paraformaldehyde in PBS for 15 min. The cells were thoroughly washed in PBS and permeabilized with 0.3% Triton-X in PBS for 5 min. The cells were then rinsed twice and incubated in a blocking buffer (10% BSA in PBS) for 1 h at room temperature. Each of the coverslips was then submerged for 30 min in 200 µl of fluorescent phalloidin in PBS (~6.6 µM) in a well of a 24-well cell culture plate. The cells were then thoroughly rinsed with PBS and mounted on a glass slide with mounting medium (Prolong Antifade kit; Molecular Probes). Fluorescently labeled actin CSK of ASM cells with surface-bound beads were examined under an epifluorescence microscope (Olympus IX70; Olympus Optical, Tokyo, Japan) and imaged by using a 1,280 × 1,024-pixel, 12-bit gray scale, and Peltier cooled monochrome charge-coupled device camera (SensiCam; Cooke, Auburn Hills, MI).

**Image analysis and quantification of actin CSK remodeling.** For a given experimental condition and time point, three to six coverslips

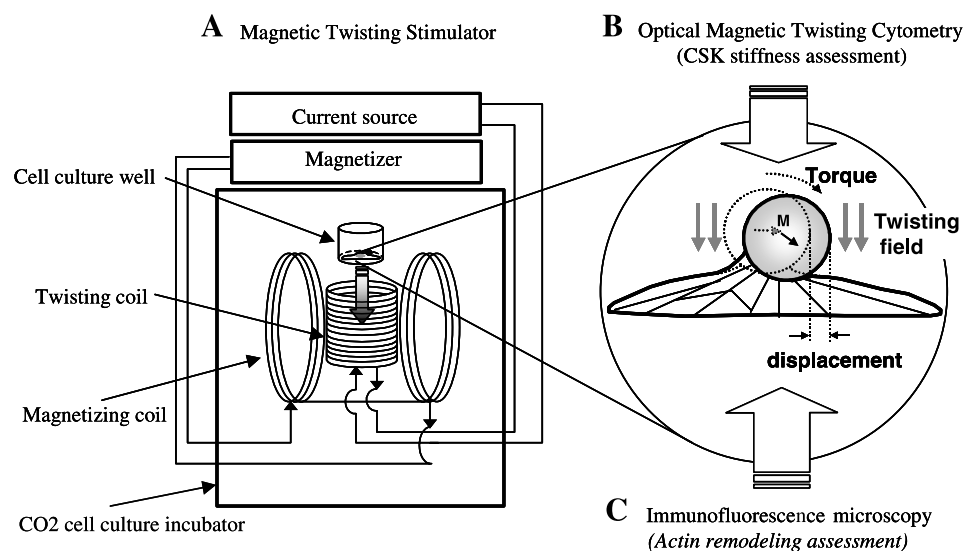


Fig. 1. A: magnetic twisting stimulator (MTS) consists of a magnetizing coil and a twisting coil inside which cultured airway smooth muscle (ASM) cells were stimulated by the oscillation of ferrimagnetic beads attached to the cells. B: optical magnetic twisting cytometry (OMTC) optically tracks and records the bead motions while magnetically oscillating the beads similar to that in MTS but under a microscope. The magnified view illustrates a ferrimagnetic bead tethered to the cytoskeleton (CSK) of a cell.  $M$ , magnetic moment of the bead initially oriented horizontally. The bead twists in response to an oscillating torque created by the application of an oscillating vertical magnetic twisting field. CSK stiffness was determined by OMTC (see text for details), and CSK remodeling from MTS was assessed by using fluorescence microscopy (C).

were prepared from repeated experiments. Coverslips with fluorescently labeled ASM cells were examined under the microscope at  $\times 100$  magnification. On average, a field of view (0.18-mm diameter) covered one to three cells, containing approximately five attached beads in total. We examined the majority of the cells on each coverslip by scanning the field of view across the coverslip and recorded images from, on average, eight randomly chosen fields of view with no overlap where there were beads attached to the cells. For a given field of view, we examined the beads attached to the cells from below. Before taking images, we manually changed the focal plane, examining the three-dimensional structures for each bead-cell attachment. To fully capture any bead-associated actin structures for each field of view, we recorded between three and five images from different focal planes  $\sim 1\text{--}2\ \mu\text{m}$  apart.

Subsequent analysis of the recorded images revealed structures of a higher actin density on and/or near some beads, indicating changes of actin CSK structure due to bead-associated actin activity. The bead was counted as positive once actin was clearly associated with the bead in any of the recorded focal planes. We thus classified the beads with associated actin structures as positive beads against those as negative that were not associated with discernible actin structures (Fig. 2, B–D). Because magnetic interference between beads can occur for beads that are clustered or that are within one bead diameter of each other, we excluded these from evaluation and examined only isolated beads, as exemplified in Fig. 2D. For each experimental condition, the total score of positive beads and negative beads was obtained. We then quantified actin CSK remodeling as the percentage of positive beads from the total number of evaluated beads, which

ranged from over 100 to several hundred for each experiment condition.

**Optical magnetic twisting cytometry.** Cytoskeletal stiffness of cultured ASM cells was measured by using optical magnetic twisting cytometry (OMTC) (Fig. 1). OMTC is similar to MTS in that it uses magnetic beads in the same manner to oscillate cell-bound beads. The magnetizing and twisting coils are smaller, however, and were fitted on a microscope stage. By optically tracking the bead motions resulting from the sinusoidal magnetic twisting, the mechanical properties of the actin CSK can be determined.

When a specific torque ( $\vec{T}$ ), as defined in Eq. 1, is applied to the bead, the ratio of the torque to the resultant bead displacement  $\vec{d}$  defines a complex stiffness  $\vec{G}$ ,

$$\vec{G} = \frac{\vec{T}}{\vec{d}} = G' + iG'' \quad (2)$$

where  $G'$  is an elastic modulus, or stiffness, of the CSK, which has units of Pascal per nanometer,  $G''$  is a loss modulus, and  $i$  is the unit imaginary number  $-1$ .  $G'$  and  $G''$  are related to the bulk storage and loss modulus of cells by a constant scaling factor ( $6.8\ \mu\text{m}$ ) via a computational model (27). In this study, we did not examine  $G''$ , which is usually 10–20% of  $G'$  (14). The displacement of beads ( $\vec{d}$ ) for the given frequency was determined from the recorded bead motions by using Fourier transformation (14, 32).

Details of OMTC have been published elsewhere (14, 32). In brief, ASM cells cultured in 6.4-mm wells were prepared with beads, as described in MTS ( $\sim 20,000$  beads per well). The cell-bead prepara-

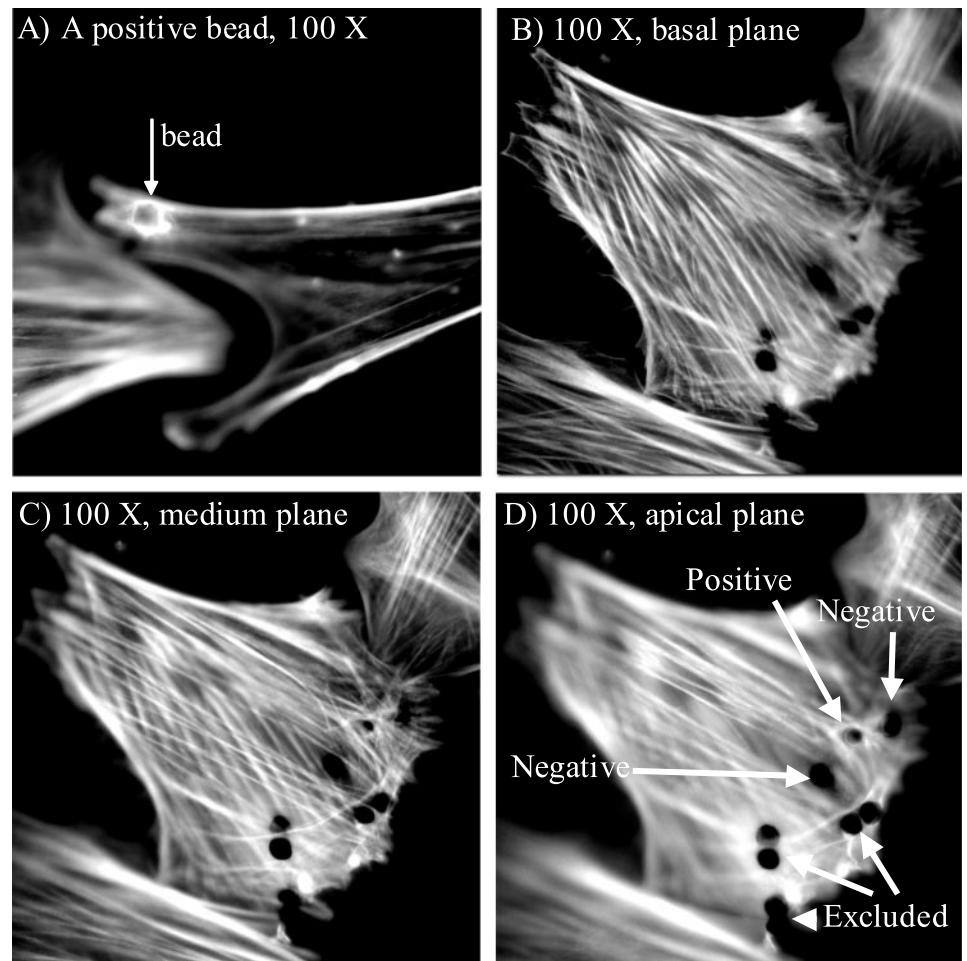


Fig. 2. Examples of fluorescently labeled actin in cultured ASM cells illustrating bead quantification technique. A: bead with strong positive bead-associated actin staining. B–D: different sectional images of an ASM cell with attached beads that scored as either positive or negative, according to the actin staining around the beads. Clustered beads were excluded from analysis, as shown in D.

tion was then placed in the twisting device fitted on the epifluorescence microscope by using a  $\times 20$  objective (numerical aperture 0.40). A specific torque identical to that in MTS but with a frequency of 0.5 Hz (limited by the camera frame rate) was applied to the beads, while the charge-coupled device camera (SensiCam, described above) imaged  $\sim 200$  beads at 16 frames per twisting cycle, phase locked to the twisting field. Bead positions on the image were determined by using an intensity centroid algorithm (14). The resolution of the OMTC was 2.5 nm (root mean square) at  $\times 20$  magnification. The displacement of beads in response to the applied torque was computed from the recorded bead positions after being digitally processed to eliminate drift and noise as well as beads with erratic, irreproducible motions (see Refs. 14 and 32 for details).

**Experimental protocol.** To assess the effects of MS on actin CSK remodeling and CSK stiffening in ASM cells, we subjected the cell-bead preparations to the mechanical stimulation of 56-Pa specific torque at 0.3 Hz, as defined in *Magnetic twisting stimulator* (referred to as MS hereafter) for up to 2 h. During that period, the beads were remagnetized every 15 min to maintain their magnetic moment and moment alignment.  $G'$  was measured after 15 min of bead binding (referred to as baseline, time  $t = 0$ ) and after mechanical stimulation at time points of  $t = 5, 15, 30, 60,$  and  $120$  min.  $G'$  was also measured in time-matched controls, where beads were added but no mechanical stimulation was delivered, except during the brief measurement period of 32 s at each time point. The actin CSK of ASM cells was imaged at identical time points but with different cell-bead preparations, as described in *Fluorescence microscopy*. To compare actin CSK changes induced by MS to actin CSK changes induced by contractile stimulation (CS), we exposed both mechanically stimulated and unstimulated cells to contractile agonists KCl (80 mM) or ACh ( $10^{-4}$  M) at doses chosen to guarantee a maximum response in  $G'$  as measured by OMTC (1, 4, 22, 28). Cells stimulated with KCl or ACh alone are referred to as KCl or ACh, respectively, whereas cells with mechanical stimulation and KCl or mechanical stimulation and ACh are referred to as KCl + MS and ACh + MS, respectively. In experiments with CS, after 15 min of initial bead binding, the cell-bead preparations were placed in an isotonic 80 mM KCl solution or  $10^{-4}$  M ACh (see *Reagents*), instead of the serum-free medium. Then the cell-bead preparations were either mechanically stimulated or not and fixed in 4% paraformaldehyde at  $t = 5, 15, 30, 60,$  and  $120$  min for KCl or at  $t = 5, 30,$  and  $60$  min for ACh. Cells were also fixed at corresponding time points without addition of KCl or ACh and without mechanical stimulation as baseline controls.

**Data processing and statistics.** The percentages of positive beads, as measured from image analysis, are given as means  $\pm 1$  SE, averaged over  $n$  repeated experiments (i.e., coverslip). For each data point (MS, controls, KCl, or MS + KCl at each time point), three to five repeated experiments were conducted ( $n = 3-5$ ), except for MS at 60 min and KCl at 15 min, when  $n = 8$  and  $9$ , respectively. The number of beads ( $N$ ) measured in each experiment ranged from 124 to 577 (mean of  $N = 299$ ). For ACh or MS + ACh, experiments were repeated eight times at each time point, resulting in the number of beads from 118 to 763 and average of 430 beads. To test for significant differences between two experiment conditions, a Student's  $t$ -test with 95% confidence level was used ( $P < 0.05$ ).

Because  $G'$  measured by OMTC was approximately log-normally distributed, results are given as median  $\pm 1$  SE. Student's  $t$ -tests were conducted on the logarithmically transformed data. We measured  $G'$  in four to six wells for each condition. Each well contained  $\sim 300$  beads, totaling roughly 1,000 beads for each condition.

**Reagents.** All chemicals were from Sigma Chemical (St. Louis, MO), unless indicated otherwise. Tissue culture reagents, including DMEM/F-12 medium and trypsin-EDTA solution, were purchased from GIBCO (Grand Island, NY). Isotonic potassium chloride solution (80 mM KCl) was prepared with 64.75 mM NaCl, 80 mM KCl, 1.2 mM  $\text{Na}_2\text{HPO}_4$ , 2 mM MOPS, 0.02 mM EDTA, 1.6 mM  $\text{CaCl}_2$ , 1.2 mM  $\text{MgSO}_4$ , and 5.6 mM glucose, dissolved in double-distilled

and sterile water. ACh was diluted to  $10^{-2}$  M in PBS as stock. We added 20  $\mu\text{l}$  of stock ACh solution to the 2-ml serum free medium in 35-mm petri dishes containing the cells, giving a final concentration of  $10^{-4}$  M.

## RESULTS

**Actin CSK remodeling in response to MS.** In ASM cells that had been mechanically stimulated for up to 2 h, we found that the percentage of beads associated with actin CSK structures (positive beads) increased with time during MS (Fig. 3). Before application of MS, only  $6.7 \pm 2.8\%$  of the beads scored positive. With MS, the number of positive beads increased to  $68.1 \pm 2.0\%$  at  $t = 60$  min and reached  $86.9 \pm 1.9\%$  at the end of 2-h stimulation. This increase was biphasic, with an initial rapid increase after the onset of MS followed by a more gradual increase at  $t > 30$  min. In the time-matched controls without MS, the number of positive beads did not change greatly over time and remained significantly smaller than in the cells exposed to MS at all time points ( $P < 0.05$ ), except at  $t = 5$  min. At  $t = 60$  min, only  $38.4 \pm 5.5\%$  of the beads scored positive in controls without MS compared with  $68.1 \pm 1.6\%$  in cells exposed to MS ( $P < 0.05$ ).

**Actin CSK remodeling in response to MS and/or CS.** In cells that were exposed to KCl, the time course of actin remodeling was similar to that of MS cells for early times ( $t = 0-30$  min, Fig. 4). However, at  $t = 60$  and  $120$  min, cells with MS scored significantly more positive beads. At 120 min,  $86.9 \pm 1.9\%$  of beads in cells with MS stained positively compared with only  $38.2 \pm 1.6\%$  in cells with KCl ( $P < 0.05$ ). Responses to ACh roughly paralleled those found with KCl, as shown in Fig. 4, *inset*. In cells that were exposed to ACh, the time course of actin remodeling was similar to that of MS cells for early times. However, like KCl, at  $t = 30$  and  $60$  min, cells with MS scored significantly more positive beads than from ACh ( $60.9 \pm 5.3$  vs.  $37.4 \pm 5.1\%$  at 30 min and  $68.7 \pm 1.6$  vs.  $60.7 \pm 2.0\%$  at 60 min;  $P < 0.05$ ). In cells receiving both MS and KCl, or both MS and ACh, there was no apparent difference in the percentage of positive beads compared with cells receiving MS alone at all times measured ( $P > 0.05$ ), except for cells with MS + KCl at  $t = 60$  min (Fig. 4).

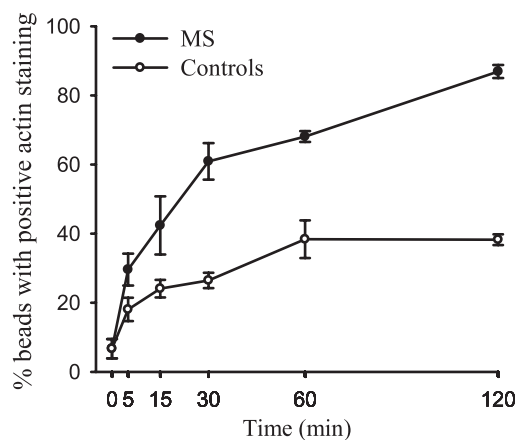


Fig. 3. Time course of actin CSK remodeling of the cultured ASM cells during mechanical stimulation (MS) (●) and in time-matched control cells (○), quantified as the percentage of beads associated with positive actin staining of the total no. of beads measured vs. duration of MS. Values are means  $\pm$  SE ( $n = 3-5$  except for MS at 60 min, where  $n = 8$ ). \* $P < 0.05$ .

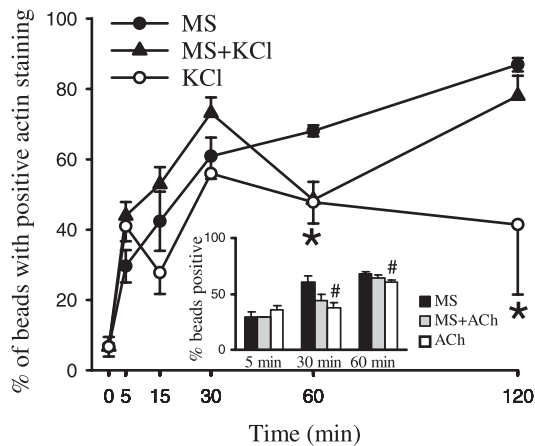


Fig. 4. Actin CSK remodeling vs. time in cultured ASM cells that had been mechanically stimulated (MS; ●) compared with that of the cells that had been stimulated by contractile activation (CS) alone with KCl (○) or MS + KCl (▲). *Inset*: actin CSK remodeling induced by MS (solid bars) compared with that by ACh (open bars) or MS + ACh (shaded bars). Values are means  $\pm$  SE;  $n = 3-5$  for MS, KCl, and MS + KCl, except for MS at 60 min ( $n = 8$ ), KCl at 15 min ( $n = 9$ ), and ACh and MS + ACh ( $n = 8$ ). \* $P < 0.05$ , MS compared with KCl; # $P < 0.05$ , MS compared with ACh.

*Actin CSK stiffening in response to MS.*  $G'$  of the ASM cells also increased with time in response to MS (Fig. 5).  $G'$  increased more than threefold ( $P < 0.05$ ), from  $0.45 \pm 0.30$  Pa/nm before MS ( $t = 0$ ) to  $1.85 \pm 0.57$  Pa/nm after 2 h of stimulation. We also observed a moderate and significant ( $P < 0.05$ ) increase of  $G'$  in the time-matched controls, from  $0.45 \pm 0.30$  Pa/nm at  $t = 0$  to  $0.93 \pm 0.29$  Pa/nm at  $t = 120$  min. The increase of  $G'$  in the control cells reached a plateau at  $\sim 30$  min, whereas the  $G'$  in the cells experiencing MS reached a plateau at  $\sim 60$  min of stimulation. At all time points  $t > 15$  min, in cells that received MS,  $G'$  was significantly higher ( $P < 0.05$ ) than in the time-matched controls.

*Actin CSK structural changes in response to MS or CS.* Bead-associated actin also displayed various features in its structure with varying intensity and extent. These features could be generally characterized as four distinctive groups, i.e., ring, filament, spindle, and halo in the order of increasing relative actin staining intensity and/or extent. Figure 6 shows representative beads with these features. Halo, spindle, and filament were strong (intensity or extent) features of actin structure that had bright intensity and/or extended away from the bead, sometimes by as much as  $10 \mu\text{m}$ , whereas the rings were generally dim and smaller than a bead diameter. Figure 7 compares the time courses of strong and ring features during exposure to either MS or CS with KCl. Beads with strong features increased persistently during MS (solid circles), whereas few beads exhibited strong features during KCl stimulation (open circles), and their number varied little except at  $t = 15$  min (Fig. 7, *left*). Ring features developed similarly during both MS and KCl (Fig. 7, *middle*). KCl induced predominantly ring features, whereas MS induced both features (comparing *left* and *middle* panels of Fig. 7). During MS, when beads showing only strong features are expressed as a percentage of all of the positively staining beads, there appears to be an increase in strong features at the expense of ring features in the first 15 min (Fig. 7, *right*).

## DISCUSSION

The principal findings of this report are as follows. We found that the application of localized oscillatory MS to cultured ASM cells by twisting integrin-bound microbeads induced progressive actin remodeling and progressive cell stiffening. We also found that contractile activation with either KCl or ACh during mechanical stimulation did not increase the actin CSK remodeling over that induced by MS alone. However, continuous mechanical stimulation over more than 30 min caused greater remodeling in the CSK than by contractile activation alone with either KCl or ACh. In the following discussion, we will first address methodological issues and compare our results to previous findings. We will then discuss possible mechanisms and implications of our results.

*Magnetic beads for study of CSK.* Various methods have been used to study cell responses to MS, including stretching cells cultured on a flexible membrane, shearing adherent cells in a flow chamber, cell poking with micropipettes, and manipulating microbeads attached to cells. Here we used magnetic beads to deliver localized MS to the CSK, as has been similarly used previously (10, 19, 25, 41). The level of mechanical stimulation that we applied is given as 56 Pa, which is the applied torque per bead volume and has a dimension of Pascal but does not represent the applied stress. Mijailovich et al. (27) have computed the stress delivered by an adherent microbead to a cell in a simulated condition similar to our technique and found the stress to be on the order of 1,000 Pa. The actual stress varies over the cell-bead contact area and depends greatly on the degree of embedment, and thus stress was heterogeneously applied in our study, necessitating assessment of a large number of beads. It is interesting to note that the level of applied MS is comparable to increases in stress found to be induced by contractile activation (42). Applying MS using adherent microbeads also allowed us to directly measure changes in CSK mechanics due to mechanical stimulation at the sites where mechanical stimulation was applied.

*Fluorescent imaging of bead-associated actin structure.* To quantify the actin CSK remodeling resulting from mechanical stimulation with magnetic beads, we imaged phalloidin-stained actin using fluorescence microscopy. A difficulty with this method is that out-of-focus light degrades the image. However, this light is diffuse, and, by adjusting the focal plane, distinct

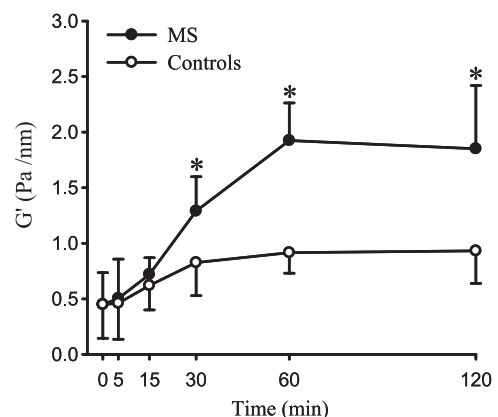


Fig. 5. Changes in CSK stiffness ( $G'$ ) of cultured ASM cells measured by OMTC vs. duration of MS (●) or time-matched controls (○). Values are medians  $\pm$  SE;  $n = 4-6$ . \* $P < 0.05$ .

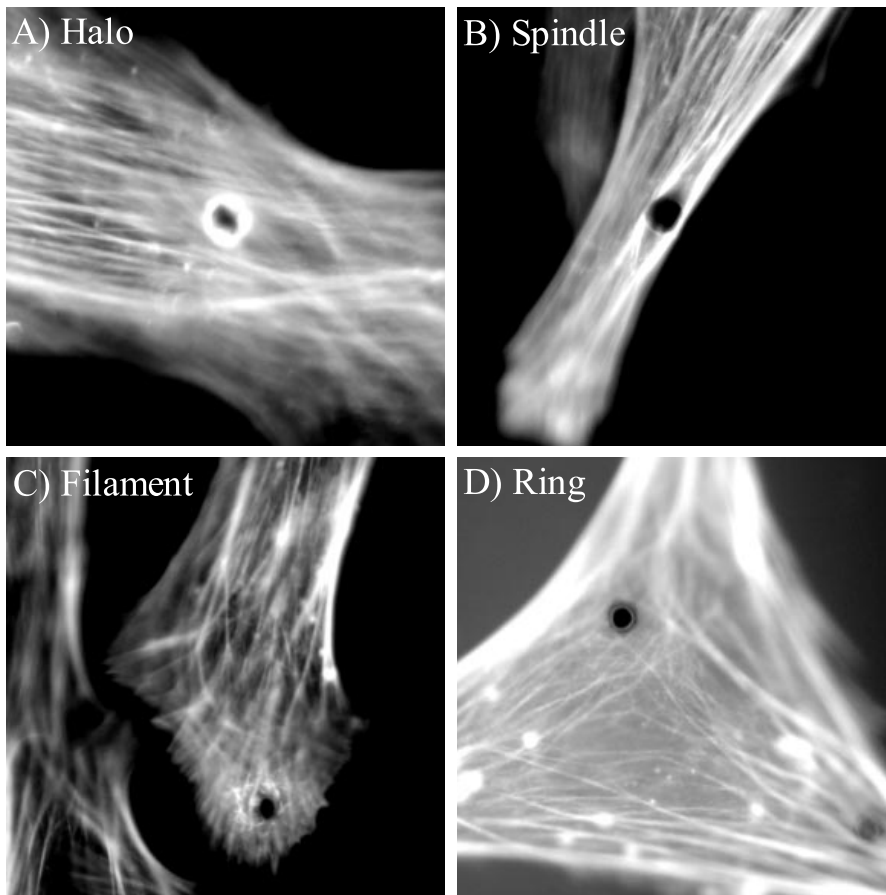


Fig. 6. Different features of bead-associated actin structure. A: halo; B: spindle; C: filament; D: ring. Features as shown in A–C were bright in fluorescent intensity, large, and/or extensive (referred to as strong features in text), compared with the ring features (D), which were dim, hairline thin, and usually smaller than a bead diameter.

bead-associated actin features could easily be discerned, and images were recorded from several vertically spaced image planes chosen to capture these features. Furthermore, subconfluent ASM cells are very thin, which reduces the contribution from out-of-plane fluorescence. It might be that dim actin structures were overlooked by our technique, but this would most likely only affect early time points of mechanical stimulation or controls. In any case, with our method, we were able to discern clear differences in actin staining intensity near beads from the background intensity within the region of one bead diameter, as demonstrated in Fig. 6 and as others have also reported with epifluorescence imaging (16, 17).

*Stiffness measurement using magnetic beads.* Optical magnetic twisting cytometry has been previously used to measure CSK  $G'$  of cultured adherent cells, including ASM cells (15, 33). This technique probes the CSK mechanical properties by optically detecting the motion of individual beads in response to an externally applied force while the beads are connected to the CSK through ligand-receptor linkages. As reported previously, we found that  $G'$  was highly heterogeneous and distributed approximately log-normally (13, 14, 25, 32). This heterogeneity has been largely attributed to differences in bead attachment characteristics, such as the number of binding sites linking the bead to the focal adhesion, and the focal adhesion

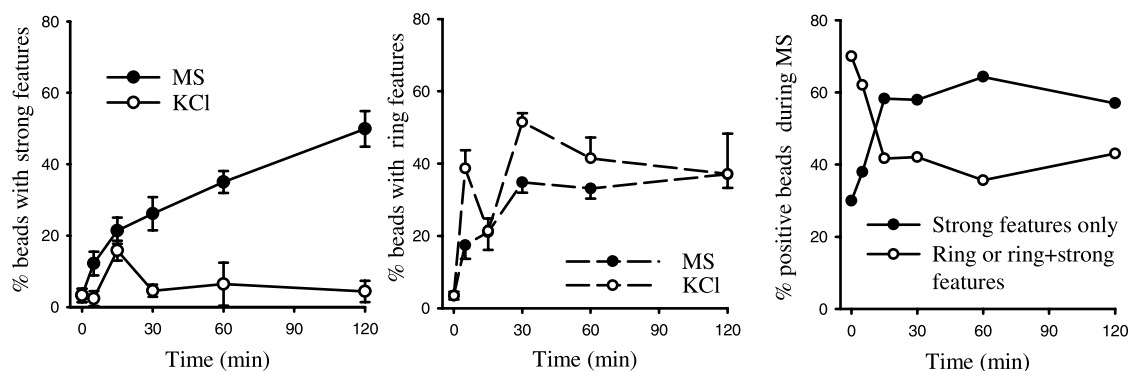


Fig. 7. Comparison of strong features and ring features during MS with those during CS with KCl. Values are means  $\pm$  SE;  $n = 3$ –5, except for MS at 60 min ( $n = 8$ ) and KCl at 15 min ( $n = 9$ ).

linkage to the CSK, but a significant portion of the heterogeneity is ascribed to variations in cell properties (14). This heterogeneity and the distribution of applied MS required that many beads (and cells) be probed to detect small  $G'$  differences (14). We measured over 300 beads for each experiment, usually repeated four to six times for each experimental condition, which provided more than a sufficient number of beads to observe significant differences.

Our results from cultured ASM cells are in general agreement with those findings from other cell types by using a variety of techniques from bead pulling to optical laser trapping. In particular, MS applied to fibroblasts and endothelial cells via surface-bound beads have been found to induce bead-associated local remodeling in CSK proteins, including actin filament accumulation and formation of focal adhesion complex containing actin, vinculin, and talin (9, 16, 17, 19). Mechanically induced stiffening in cells has also been reported to be associated with remodeling in the CSK (10, 16). Our results are consistent with these findings and extend them. We demonstrate quantitatively that localized MS induced actin remodeling in a time-dependent manner, correlated with the increasing  $G'$  of the CSK. Furthermore, MS induced a more than twofold increase in  $G'$ , greater than that caused by contractile activation, as discussed below.

*Contractile activation vs. MS.* Contractile activation is known to stimulate actin polymerization in ASM (26) and increase the stiffness of ASM cells, due partly to increased actin polymerization and partly to enhanced actomyosin activity (1, 22). We used the contractile agonists KCl and ACh at doses chosen to evoke maximal changes in ASM cell  $G'$  and compared responses between contractile and mechanical stimulation. Both agonists increased bead-associated actin polymerization rapidly within 5 min, followed by a somewhat lower increase due to ACh by 30 min compared with KCl at 30 min (ACh  $37.4 \pm 5.1\%$  vs. KCl  $56.0 \pm 1.5\%$ ;  $P < 0.05$ ), and both reached comparable levels at 60 min (ACh  $60.1 \pm 1.9\%$  vs. KCl  $47.8 \pm 1.9\%$ ;  $P > 0.05$ ). Actin remodeling was comparable for both agonists and MS at early times. Although other contractile agonists may lead to different levels of actin polymerization, with the two agonists we employed, less bead-associated actin polymerization was found than with mechanical stimulation at times  $>30$  min. Although the volume of agonist was very large compared with the cell number, such that dilution with time was unlikely, the lower response due to CS may be due, in part, to the effect of decreasing effectiveness of the contractile agonists. However, reports measuring stiffness changes by using magnetic beads found increases in stiffness in ASM cells, varying from 30 to 70% due to a variety of contractile agonists, including KCl and ACh (1, 22, 25, 42). Here we found that MS caused a greater increase in  $G'$  than in these studies, and that these changes in  $G'$  due to MS were well correlated with observed CSK remodeling in response to MS. That the increase we found with MS was greater than those reported with CS is also well correlated with the greater bead-associated CSK remodeling that we found with MS compared with CS, as we observed. Furthermore, the combination of MS and contractile agonist (KCl + MS or ACh + MS) did not produce any further increase in actin CSK remodeling than that induced by MS alone. Taken together, these data indicate that MS is a potent stimulus for CSK remodeling compared with contractile activation. Indeed, it may be that

some of the actin polymerization that we and others observed (1, 22, 26) during CS could be a result of increased stress within the CSK that is brought about by actin-myosin activity. However, we cannot conclude that MS alone, in the absence of contractile activation, can induce increased actin polymerization. The contractile machinery of ASM cells in culture is partially activated (22, 25), and it may be that this contributed to the CSK stiffening and remodeling in ASM cells that we observed. Nevertheless, that MS is such a potent stimulus for increasing CSK stiffness in ASM has important physiological implications, as discussed below.

*Actin structures.* We found that the number of beads staining positive for bead-associated actin structures increased dramatically with the application of MS. However, we also observed that the intensity and extent of actin structures around the beads also appeared to change during exposure to MS. As shown in Fig. 6, markedly different structures formed near the beads. It was interesting to group them into four characteristic features that we termed ring, filament, spindle, and halo in the order of increasing relative actin staining intensity, which we further separated into two classes, larger actin structures, which we termed strong, and hairline ring actin structures, which we termed ring. These structures were not necessarily exclusive of each other, and a combination of different structures was occasionally present on a single positive bead. For example, some of the beads with ring features also showed strong features; of the positively staining beads during MS,  $<7\%$  (30 min) and  $<16\%$  (120 min) showed both ring features and strong features. We did this because measuring the positive beads alone did not account for changes of these structures or differences due to MS and contractile stimuli. We thus compared the changes of either strong features or ring features on positive beads in response to stimulation.

An interesting pattern emerged. Greater numbers of strong actin structures were caused by MS compared with KCl, which continued to increase with duration of MS (Fig. 7, *left*). On the other hand, ring features responded similarly to either MS or KCl (Fig. 7, *middle*) or ACh (data not shown). The large actin structures that appeared in MS-stimulated cells over time may have been partly due to growth of ring structures into strong features, as indicated by the changing percentage of ring and strong features among the positively stained beads (Fig. 7, *right*). Interestingly, the formation of strong actin structures caused by either KCl or ACh was rare, never exceeding 23% of the positive beads at any time examined.

Thus MS appeared to elicit the formation of larger, more intense, and more complex actin features, whereas CS involved a more modest response with a lack of development in those strong structures. This was also borne out in time-matched controls, where only 11% of the beads that stained positively for actin showed evidence of strong features. The increase in larger features due to MS compared with time-matched controls and, compared with CS, agreed with the greater increase in  $G'$  due to MS.

*Mechanisms for stress-induced CSK remodeling and stiffening.* The mechanisms by which MS induces and regulates changes in CSK structure and function are unclear. It has been proposed that MS applied to the cell via ligand-integrin linkage may result in geometric distortion in CSK components, changing their physiochemical properties locally, and create a milieu that is possibly preferable to actin assembly (23). On the other

hand, it may be that MS may regulate actin assembly through protein-protein bond formation and kinetics (2). Possibly, MS may also activate stress-sensitive ion channels to trigger a transient increase of calcium influx, leading to a raised gradient of calcium near a bead (18, 30), and thus causing local actin polymerization (39). Stress also causes activation of focal adhesion proteins, such as FAK and paxillin (33), which could perhaps affect actin fiber polymerization. Each of these mechanisms may contribute to the increase of actin accumulation at the beads during mechanical stimulation.

Our aggregate data show that larger, more diverse actin structures appear to evolve from ring structures that formed early in either MS- or CS-stimulated cells, and larger structures occurred much more commonly in response to MS compared with CS. Whereas the mechanisms for the different behavior are unknown, CS involves the activation of contractile pathways throughout the cells, resulting in continuous increased cell stress, whereas MS involves cyclic loading localized at focal adhesions. Thus, although MS and CS both increase stress that resulted in increased bead-associated actin, the stimuli are quite different and likely differently transduced.

Here we have shown that actin CSK structure and  $G'$  changed progressively in response to up to 2 h of mechanical stimulation. Our laboratory (32, 34) has also shown previously that ASM cells undergo changes in CSK contents and functions, consistent with the present findings, with longer periods (2–12 days) of mechanical stimulation. Taking both observations together, we speculate that the early effects caused by MS, as we observed in this study, may subsequently lead to increased proliferation, enhanced contractility, and greater force production and shortening velocity, as well as ablated response to relaxant as the mechanical stimulation is prolonged (35–38).

**Physiological implications.** The ability of the ASM CSK to rapidly remodel and stiffen in response to MS may have important implications to airway function and pathology, particularly in diseases such as asthma, where MS might be increased due to wheeze, increased inspiratory efforts, and exacerbations. Mechanically induced CSK remodeling may affect ASM function by altering force generation and normal regulation of the CSK structure. Indeed, the reorganization of the CSK is now strongly believed to be a normal feature of ASM function through several postulated mechanisms (15, 20, 31). Thus changes in the CSK due to mechanical stimulation may compromise or modulate these behaviors. Furthermore, enhanced stiffness may contribute to impaired dilation of constricted airways observed in asthma. Once constricted, airways of asthmatic subjects do not remain dilated after a deep inspiration, but rather narrow again (7). Enhanced stiffness could provide a plausible mechanism for maintained narrowed airways through increased elastic recoil.

In conclusion, we found that MS was a potent stimulus for promoting actin CSK remodeling in cultured ASM cells, thereby causing CSK stiffening. The capacity of the ASM cell to remodel its internal structures and increase its stiffness may have important consequences in asthma, where heightened MS are potentially prevalent. However, we do not imply that MS alone is sufficient for altered ASM behavior in asthma, as MS is inherent in the airways due to the action of breathing. Other factors must also contribute to ASM pathology with MS, such

as inflammation, airway wall remodeling, and elevated bronchial tone, which are associated with asthmatic airways.

#### ACKNOWLEDGMENTS

We are grateful to Dr. Jeffrey Fredberg, Harvard School of Public Health, Boston, MA, for the ferrimagnetic beads and helpful discussion. We thank Darren Cole for help preparing the cells.

#### GRANTS

This study was supported by a Whitaker Foundation Research Grant, National Heart, Lung, and Blood Institute Grant HL-65960, the Canadian Foundation for Innovation, and the Nova Scotia Health Research Foundation. N. J. Fairbank is supported by Canadian Institutes of Health Research Strategic Training Fellowship STP-53877.

#### REFERENCES

1. An SS, Laudadio RE, Lai J, Rogers RA, and Fredberg JJ. Stiffness changes in cultured airway smooth muscle cells. *Am J Physiol Cell Physiol* 283: C792–C801, 2002.
2. Asthagiri AR and Lauffenburger DA. Bioengineering models of cell signaling. *Annu Rev Biomed Eng* 2: 31–53, 2000.
3. Barnes PJ. Pharmacology of airway smooth muscle. *Am J Respir Crit Care Med* 158: S123–S132, 1998.
4. Bergner A and Sanderson MJ. Acetylcholine-induced calcium signaling and contraction of airway smooth muscle cells in lung slices. *J Gen Physiol* 119: 187–198, 2002.
5. Black JL, Roth M, Lee J, Carlin S, and Johnson PR. Mechanisms of airway remodeling. Airway smooth muscle. *Am J Respir Crit Care Med* 164: S63–S66, 2001.
6. Brackel HJ, Pedersen OF, Mulder PG, Overbeek SE, Kerrebijn KF, and Bogaard JM. Central airways behave more stiffly during forced expiration in patients with asthma. *Am J Respir Crit Care Med* 162: 896–904, 2000.
7. Brown RH and Mitzner W. Invited Review: Understanding airway pathophysiology with computed tomography. *J Appl Physiol* 95: 854–862, 2003.
8. Chen J, Fabry B, Schiffrin EL, and Wang N. Twisting integrin receptors increases endothelin-1 gene expression in endothelial cells. *Am J Physiol Cell Physiol* 280: C1475–C1484, 2001.
9. Chicurel ME, Singer RH, Meyer CJ, and Ingber DE. Integrin binding and mechanical tension induce movement of mRNA and ribosomes to focal adhesions. *Nature* 392: 730–733, 1998.
10. Choquet D, Felsenfeld DP, and Sheetz MP. Extracellular matrix rigidity causes strengthening of integrin-cytoskeleton linkages. *Cell* 88: 39–48, 1997.
11. Draeger A, Amos WB, Ikebe M, and Small JV. The cytoskeletal and contractile apparatus of smooth muscle: contraction bands and segmentation of the contractile elements. *J Cell Biol* 111: 2463–2473, 1990.
12. Dulin NO, Fernandes DJ, Dowell M, Bellam S, McConville J, Lakser O, Mitchell R, Camoretti-Mercado B, Kogut P, and Solway J. What evidence implicates airway smooth muscle in the cause of BHR? *Clin Rev Allergy Immunol* 24: 73–84, 2003.
13. Fabry B, Maksym GN, Hubmayr RD, Butler JP, and Fredberg JJ. Implications of heterogeneous bead behavior on cell mechanical properties measured with magnetic twisting cytometry. *J Magnetism Magnetic Materials* 194: 120–125, 1999.
14. Fabry B, Maksym GN, Shore SA, Moore PE, Panettieri RA Jr, Butler JP, and Fredberg JJ. Selected contribution: time course and heterogeneity of contractile responses in cultured human airway smooth muscle cells. *J Appl Physiol* 91: 986–994, 2001.
15. Fredberg JJ, Inouye DS, Mijailovich SM, and Butler JP. Perturbed equilibrium of myosin binding in airway smooth muscle and its implications in bronchospasm. *Am J Respir Crit Care Med* 159: 959–967, 1999.
16. Galbraith CG, Yamada KM, and Sheetz MP. The relationship between force and focal complex development. *J Cell Biol* 159: 695–705, 2002.
17. Glogauer M, Arora P, Chou D, Janmey PA, Downey GP, and McCulloch CA. The role of actin-binding protein 280 in integrin-dependent mechanoprotection. *J Biol Chem* 273: 1689–1698, 1998.
18. Glogauer M, Arora P, Yao G, Sokholov I, Ferrier J, and McCulloch CA. Calcium ions and tyrosine phosphorylation interact coordinately with actin to regulate cytoprotective responses to stretching. *J Cell Sci* 110: 11–21, 1997.

19. **Glogauer M and Ferrier J.** A new method for application of force to cells via ferric oxide beads. *Pflügers Arch* 435: 320–327, 1998.
20. **Gunst SJ and Wu MF.** Selected contribution: plasticity of airway smooth muscle stiffness and extensibility: role of length-adaptive mechanisms. *J Appl Physiol* 90: 741–749, 2001.
21. **Hirshman CA and Emala CW.** Actin reorganization in airway smooth muscle cells involves  $G_q$  and  $G_{i-2}$  activation of Rho. *Am J Physiol Lung Cell Mol Physiol* 277: L653–L661, 1999.
22. **Hubmayr RD, Shore SA, Fredberg JJ, Planus E, Panettieri RA Jr, Moller W, Heyder J and Wang N.** Pharmacological activation changes stiffness of cultured human airway smooth muscle cells. *Am J Physiol Cell Physiol* 271: C1660–C1668, 1996.
23. **Ingber DE.** Tensegrity II. How structural networks influence cellular information processing networks. *J Cell Sci* 116: 1397–1408, 2003.
24. **King GG, Pare PD, and Seow CY.** The mechanics of exaggerated airway narrowing in asthma: the role of smooth muscle. *Respir Physiol* 118: 1–13, 1999.
25. **Maksym GN, Fabry B, Butler JP, Navajas D, Tschumperlin DJ, Laporte JD, and Fredberg JJ.** Mechanical properties of cultured human airway smooth muscle cells from 0.05 to 04 Hz. *J Appl Physiol* 89: 1619–1632, 2000.
26. **Mehta D and Gunst SJ.** Actin polymerization stimulated by contractile activation regulates force development in canine tracheal smooth muscle. *J Physiol* 519: 829–840, 1999.
27. **Mijailovich SM, Kojic M, Zivkovic M, Fabry B, and Fredberg JJ.** A finite element model of cell deformation during magnetic bead twisting. *J Appl Physiol* 93: 1429–1436, 2002.
28. **Mitchell RW, Halayko AJ, Kahrman S, Solway J, and Wylam ME.** Selective restoration of calcium coupling to muscarinic M(3) receptors in contractile cultured airway myocytes. *Am J Physiol Lung Cell Mol Physiol* 278: L1091–L1100, 2000.
29. **Naghshin J, Wang L, Pare PD, and Seow CY.** Adaptation to chronic length change in explanted airway smooth muscle. *J Appl Physiol* 95: 448–453, 2003.
30. **Pommerenke H, Schreiber E, Durr F, Nebe B, Hahnel C, Moller W, and Rychly J.** Stimulation of integrin receptors using a magnetic drag force device induces an intracellular free calcium response. *Eur J Cell Biol* 70: 157–164, 1996.
31. **Pratusevich VR, Seow CY, and Ford LE.** Plasticity in canine airway smooth muscle. *J Gen Physiol* 105: 73–94, 1995.
32. **Smith PG, Deng L, Fredberg JJ, and Maksym GN.** Mechanical strain increases cell stiffness through cytoskeletal filament reorganization. *Am J Physiol Lung Cell Mol Physiol* 285: L456–L463, 2003.
33. **Smith PG, Garcia R, and Kogerman L.** Mechanical strain increases protein tyrosine phosphorylation in airway smooth muscle cells. *Exp Cell Res* 239: 353–360, 1998.
34. **Smith PG, Garcia R, and Kogerman L.** Strain reorganizes focal adhesions and cytoskeleton in cultured airway smooth muscle cells. *Exp Cell Res* 232: 127–136, 1997.
35. **Smith PG, Janiga KE, and Bruce MC.** Strain increases airway smooth muscle cell proliferation. *Am J Respir Cell Mol Biol* 10: 85–90, 1994.
36. **Smith PG, Moreno R, and Ikebe M.** Strain increases airway smooth muscle contractile and cytoskeletal proteins in vitro. *Am J Physiol Lung Cell Mol Physiol* 272: L20–L27, 1997.
37. **Smith PG, Roy C, Dreger J, and Brozovich F.** Mechanical strain increases velocity and extent of shortening in cultured airway smooth muscle cells. *Am J Physiol Lung Cell Mol Physiol* 277: L343–L348, 1999.
38. **Smith PG, Roy C, Fisher S, Huang QQ, and Brozovich F.** Selected contribution: mechanical strain increases force production and calcium sensitivity in cultured airway smooth muscle cells. *J Appl Physiol* 89: 2092–2098, 2000.
39. **Tang JX, Kas JA, Shah JV, and Janmey PA.** Counterion-induced actin ring formation. *Eur Biophys J* 30: 477–484, 2001.
40. **Valberg PA and Butler JP.** Magnetic particle motions within living cells. Physical theory and techniques. *Biophys J* 52: 537–550, 1987.
41. **Wang N, Butler JP, and Ingber DE.** Mechanotransduction across the cell surface and through the cytoskeleton. *Science* 260: 1124–1127, 1993.
42. **Wang N, Tolic-Norrelykke IM, Chen J, Mijailovich SM, Butler JP, Fredberg JJ, and Stamenovic D.** Cell prestress. I. Stiffness and prestress are closely associated in adherent contractile cells. *Am J Physiol Cell Physiol* 282: C606–C616, 2002.